A&A 403, 179–185 (2003)
DOI: 10.1051/0004-6361:20030322

Astronomy & Astrophysics

Structure of the magnetic field in the Ap star HD 187474

V. R. Khalack[1], J. Zverko[2], and J. Žižňovský[2]

[1] Main Astronomical Observatory, 27 Zabolotnogo Str., 03680, Kyiv, Ukraine
and Isaac Newton Institute of Chile, Kiev Branch
[2] Astronomical Institute of the SAS, 05960 Tatranská Lomnica, The Slovak Republic

Received 29 July 2002 / Accepted 21 February 2003

Abstract. We reconstruct the complex magnetic field in the Ap star HD 187474 within the frame of the point field source model, where virtual magnetic charges are distributed in the stellar body. The best-fit model describes sufficiently well the observed nonsinusoidal variability of the mean magnetic field modulus and the sinusoidal behaviour of the mean longitudinal magnetic field with the phase of stellar rotation. The best fit provides discrepancy on the level of $\chi^2 = 6.10$ for all the analyzed data. We show that in HD 187474 the magnetic dipole is displaced from centre of the star by 0.055 $R_\star$. The dipole has a size ~0.035 $R_\star$. The angle between the stellar rotational axis and the magnetic dipole is $\beta = 37°$.

Key words. stars: chemically peculiar – stars: magnetic fields – stars: rotation – stars: individual: HD 187474

1. Introduction

Among the magnetic Ap stars HD 187474 (V3961 Sgr, HR 7552) belongs to the group of the slowest rotators, since it has an extraordinarily long rotation period $P = 2345\,\mathrm{d} \pm 15\,\mathrm{d}$ (~6.4 yr) derived from measurements of the longitudinal magnetic field by Mathys (1991) and confirmed by Hensberge (1993) from photometric observations. This star has spent a 0.69 fraction of its main-sequence lifetime, as may be deduced from the corresponding evolutionary tracks (Hubrig et al. 2000; Schaller et al. 1992). At a distance of $d = 104.0 \pm 9.3$ parsecs (HIPPARCOS Catalogue 1997), HD 187474 is a member of a spectroscopic binary system with eccentricity $e = 0.45$ and orbital period $P_{\rm orb} = 690\,\mathrm{d}$ (Leeman 1964; Budaj 1999). It is remarkable that the rotational period greatly exceeds the period of orbital revolution.

HD 187474 is classified as A0 EuCrSr and shows strong variability of Cr, Mn, Fe, Si, Nd and Pr lines with stellar rotation. Didelon (1987) discovered Zeeman splitting of spectral lines in its spectrum and derived a mean magnetic field modulus of 5.1 kG at the rotational phase $\varphi = 0.98$. Surface abundance of all the above mentioned chemical elements was recently derived by Strasser et al. (2001). The mapping was performed in the frame of a three-ring model of abundance distribution, introducing magnetic field as an axisymmetric low-order multipole (Landstreet & Mathys 2000).

The last decade was marked by extensive observations of the mean values (averaged over the visible hemisphere) of the surface longitudinal magnetic field (Mathys 1991), crossover effect (Mathys 1995a), the mean quadratic field (Mathys 1995b) and the magnetic field modulus (Mathys et al. 1997).

Based on these observational data, the surface structure of the magnetic field of HD 187474 was recently modelled by Landstreet & Mathys (2000). They represented the field as a superposition of centered co-linear magnetic dipole, quadrupole and octupole. This model operates with six free parameters (zero phase of stellar rotation ϕ_0, angle of inclination of the rotational axis to the line of sight, i, and dipole axis, β, with corresponding polar strengths of the dipole, $B_{\rm d}$, quadrupole $B_{\rm q}$, octupole $B_{\rm oct}$). The model, as shown by Landstreet & Mathys, accurately reproduces the observed sinusoidal behavior of the variable magnetic field for the majority of CP stars. Nevertheless, in the case of HD 187474 this approach can provide only a general, first-oder description of the surface magnetic field (Landstreet & Mathys 2000).

The complex behavior of the magnetic field of HD 187474 calls for a more flexible approach. For example, Bagnulo et al. (2002) used the oblique rotator model with a dipole plus nonlinear quadrupole field for reconstruction of the surface magnetic field configuration in HD 187474. In this paper, we explore the model with *point-like magnetic sources* embedded in the stellar body (Khalack et al. 2001a), thus fixing size(s) and location(s) of the real magnetic dipole (dipoles). The main results obtained from these two models are compared in Sect. 2.3.

2. Magnetic field reconstruction

2.1. Methodology of modelling

Recently, Gerth & Glagolevskij (1997) applied the method of *the magnetic charge description* (MCD) to model magnetic field at the stellar surface. Its advantage is in avoiding the

Send offprint requests to: V. R. Khalack,
e-mail: khalack@mao.kiev.ua

constraints on the number and the spatial distribution of sources (*magnetic charges*) provided that the total magnetic charge is equal to zero. However, for correct determination of the model's free parameters, the number of sources should be as small as possible (Khalack et al. 2001a).

Here, aiming at the precise reconstruction of the surface magnetic field in HD 187474, we apply model of a magnetic dipole, mathematically formulated with help of two virtual magnetic charges arbitrarily located in the stellar interior. Detailed description of this model is given in Appendix A. It should be noted that this approach is valid only if one attempts to reproduce the strength of magnetic field outside the volume in which the magnetic charges are embedded (Khalack et al. 2001a). Under such conditions the magnetic lines are not discontinued within the spatial range of the model, and configuration of the magnetic field produced by dipole will be equivalent to the field generated by two separated virtual magnetic charges.

Reconstruction of the surface magnetic field was based on the observations of the mean longitudinal field B_z and the mean magnetic field modulus B_s only (see Fig. 1). These data have relatively small errors of measurements, contrary to the relatively high measurement errors of the crossover effect B_c and the so called mean quadratic magnetic field B_{mq}. Small measurement errors of the initial data lead to high precision (low estimation errors) of the free model parameters.

The dependencies of the mean longitudinal field, the magnetic field modulus, as well as the crossover effect and quadratic magnetic field from the phase of stellar axial rotation do not depend on the positional angle Ω (Khalack et al. 2001b). Therefore, without a loss of generality, we can set $\Omega = 0^\circ$ in the subsequent calculations.

Following Landstreet & Mathys (2000), we weight the various magnetic field characteristics over the visible hemisphere by a product of the limb darkening and the line weakening of the form

$$W = [1 - u_c(1 - \cos\theta)][1 - u_l(1 - \cos\theta)], \quad (1)$$

where u_c and u_l are the limb darkening and the line weakening coefficients, respectively. Here θ is the same as in (A.1). It specifies the angle between the local normal to the stellar surface and the line of sight. Landstreet & Mathys (2000) have determined the mean values of $u_c = 0.4$ and $u_l = 0.5$ by calculating continuum intensities and line depths for a sample Fe II line at 6150 Å, at various values of θ, for a series of effective temperatures (from 7500 to 10 000 K). Respectively, this is also applicable in our case, to analyse the magnetic field data, which have been derived from the polarized and unpolarized spectra centered around 6000 Å (Mathys 1991; Mathys et al. 1997), for the effective temperature and surface gravity of HD 187474, $T_{\rm eff} = 10\,090 \pm 180$ K, $\log g = 3.94 \pm 0.09$ (Hubrig et al. 2000).

Therefore, after tabulating the variables u_c, u_l and Ω, one may introduce in the subsequent simulation only eight free model parameters (see Eq. (A.5)). Initially we arbitrarily place these remaining free parameters in the range of their possible values (a zero-point choice in the space of searched parameters) and then estimate the agreement between the modelled and observed dependencies of the longitudinal magnetic field and the surface magnetic field modulus from the phase of stellar rotation using a χ^2 function of the form

$$\chi^2 = \frac{1}{2}\left(\chi_z^2 + \chi_s^2\right), \quad (2)$$

where

$$\begin{cases} \chi_z^2 = \dfrac{1}{N_z}\displaystyle\sum_{i=1}^{N_z}\left(\dfrac{B_{z,i}^{obs} - B_z(\varphi_i)}{\sigma\left[B_{z,i}^{obs}\right]}\right)^2; \\ \chi_s^2 = \dfrac{1}{N_s}\displaystyle\sum_{i=1}^{N_s}\left(\dfrac{B_{s,i}^{obs} - B_s(\varphi_i)}{\sigma\left[B_{s,i}^{obs}\right]}\right)^2. \end{cases} \quad (3)$$

Here $B_{z,i}^{obs}$ and $B_{s,i}^{obs}$ are the observed mean longitudinal magnetic field and mean surface magnetic field modulus with the measurements error $\sigma[B_{z,i}^{obs}]$ and $\sigma[B_{s,i}^{obs}]$, respectively, defined for the rotational phase φ_i, while $N_z = 52$ and $N_s = 38$ are the numbers of observations.

In order to achieve the best agreement of the simulated and observed data we minimize the χ^2-function (2) with help of the *downhill simplex method* (Press et al. 1992) varying possible values of the free model parameters. The advantage of this method is that it requires the function evaluations only, but not their derivatives (Neldar & Mead 1965). This is important for the considered model, where the derivatives may have a complex form, as follows from (A.1), and should be integrated over the visible hemisphere too. Poor efficiency of the downhill simplex method in terms of the large number of function evaluations is a well known problem. Nevertheless, it always converges to a minimum (Press et al. 1992). In our case, this technique requires a comparatively long computational time, as the number of free parameters is large.

The process of minimization was performed few times, starting from different zero-points in the space of free model parameters in order to avoid possible local minima of the χ^2-function. In the case of HD 187474, the downhill simplex method converges to a few minima. Preference was given to the deepest global minimum.

In order to define the errors of modelling, we calculated the deviations of the simulated B_z and B_s, that appear as a result of varying by a certain step each of the free parameters, thus introducing a shift along the χ^2 hypersurface axis from the point of the function minimum value. Thereby, taking into account uncertainties of the observational data and the obtained minimal value of χ^2-function and using the least square method, we can estimate the errors of the best-fit parameters.

2.2. Results of reconstruction

Reconstruction of the surface magnetic field was carried out relying on the observations of the mean longitudinal magnetic field (Mathys 1991; Mathys & Hubrig 1997) and the mean surface magnetic field modulus (Didelon 1987; Mathys et al. 1997; Landstreet & Mathys 2000), which are marked correspondingly on the upper panels of Fig. 1. The data show relatively low errors of measurement, which allows to estimate the free parameters of the best-fit model with a reasonable accuracy, thus reaching a minimum of the χ^2-function (2).

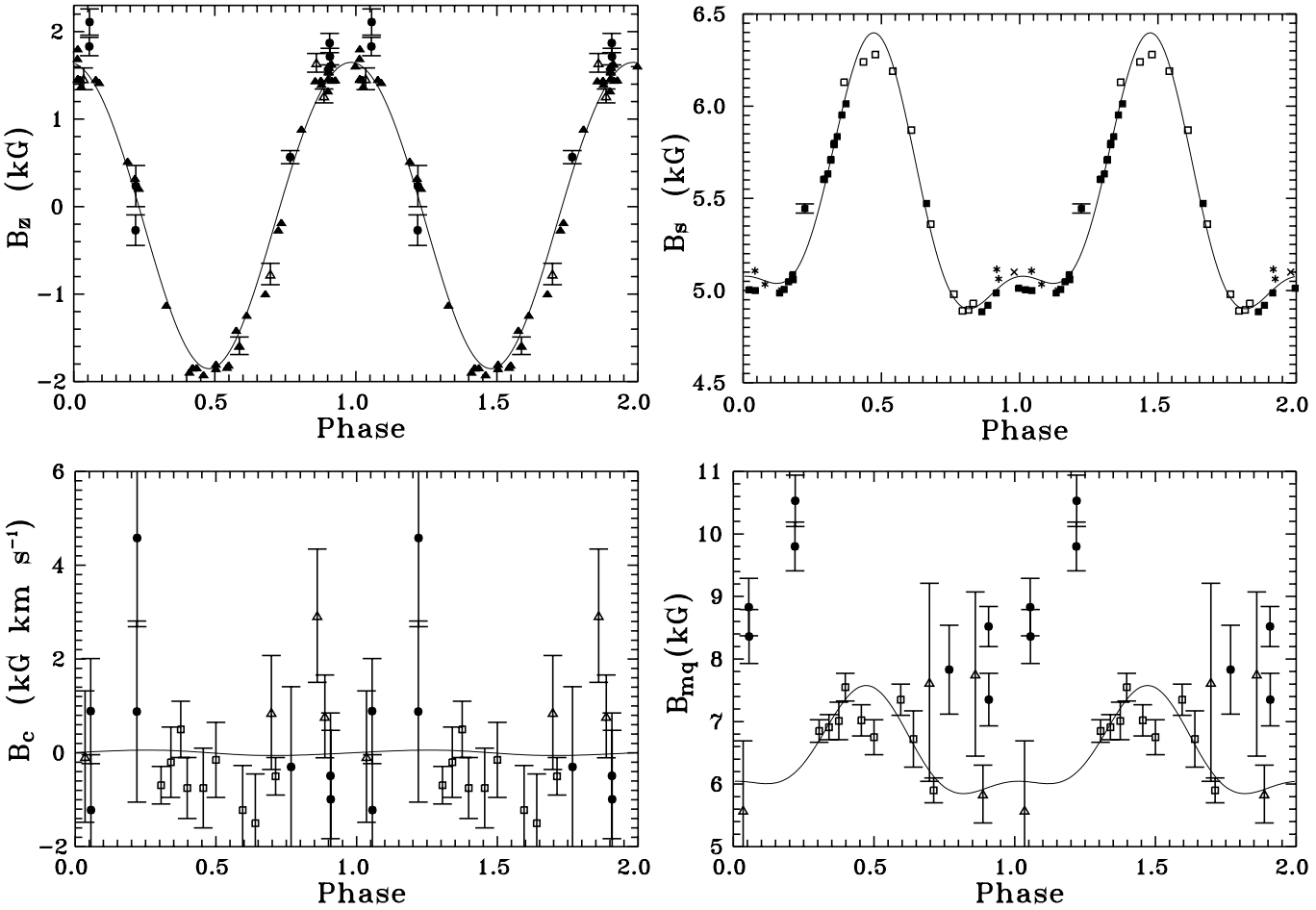

Fig. 1. Observations of HD 187474 and the best data fit obtained in the frame of the model (solid line), with the parameters given in (4). The upper two panels show the mean longitudinal magnetic field B_z and the mean magnetic field modulus B_s. The bottom two panels show the mean crossover effect B_c and the mean quadratic magnetic field B_{qm}. Filled circles: Mathys (1991, 1995a, 1995b); open triangles: (Mathys & Hubrig 1997); filled triangles: Babcock data given in (Mathys 1991); filled squares: (Mathys et al. 1997); open squares: (Landstreet & Mathys 2000); asterisks: B_s data by (Mathys et al. 1997) but obtained with a different instrumental configuration; cross: Didelon (1987).

On the contrary, the observations of the crossover effect (Mathys 1995a; Mathys & Hubrig 1997; Landstreet & Mathys 2000) and the mean quadratic magnetic field (Mathys 1995b; Mathys & Hubrig 1997; Landstreet & Mathys 2000) have relatively large measuring errors (see Fig. 1, lower panels), and were not taken into account in the simulation. Nevertheless, the observed data of the two last surface magnetic field characteristics are plotted together with the simulated curves of variability in order to estimate the general agreement between the simulated and all the available observational data.

On the basis of all mentioned data of the mean longitudinal magnetic field and magnetic field modulus, we have obtained the following values of parameters in the best-fit model

$$\begin{cases} B_0 = 161 \pm 18\ \mathrm{kG}; & i = 89^\circ \pm 5^\circ; \\ a_1 = 0.042 \pm 0.002; & a_2 = 0.070 \pm 0.003; \\ \lambda_1 = 197^\circ \pm 6^\circ; & \delta_1 = 6^\circ \pm 18^\circ; \\ \lambda_2 = 193^\circ \pm 3^\circ; & \delta_2 = 27^\circ \pm 5^\circ, \end{cases} \quad (4)$$

where B_0 defines the relation of the magnetic charge value to square of the stellar radius (A.5), i specifies inclination of the rotational axis to the line of sight, a_1 and a_2 are the distances of magnetic charges from the centre of the star, expressed in units of stellar radius, while (λ_1, δ_1) and (λ_2, δ_2) are their angular coordinates in the spherical reference frame related to the star. This set (4) of parameters in the best-fit model gives the minimum value of $\chi^2 = 6.10$. (For comparison, we also provide the values for $\chi^2_z = 5.63$ and $\chi^2_s = 6.58$.) The comparatively high errors of B_0 and δ_1 (that also involves the quality of the best fit via χ^2-function) result in a weak model response to the small changes of these parameters for a given configuration of the surface magnetic field.

We note that, due to the spherical symmetry of the model, the same value of χ^2 could be obtained with other sets of parameters

$$\begin{aligned} &a)\ \{B_0, i, \delta_1, \delta_2, \lambda_1, \lambda_2, \Omega, a_1, a_2, u_c, u_l\}; \\ &b)\ \{B_0, 180^\circ - i, -\delta_1, -\delta_2, \lambda_1, \lambda_2, \Omega, a_1, a_2, u_c, u_l\}; \\ &c)\ \{B_0, i, \delta_1, \delta_2, 360^\circ - \lambda_1, 360^\circ - \lambda_2, \Omega, a_1, a_2, u_c, u_l\}; \\ &d)\ \{B_0, 180^\circ - i, -\delta_1, -\delta_2, 360^\circ - \lambda_1, 360^\circ - \lambda_2, \Omega, \\ &\quad a_1, a_2, u_c, u_l, \} \end{aligned} \quad (5)$$

which produce the same variability of the mean longitudinal field and the surface field modulus with the phase of stellar rotation. In (5) the cases a and c differ from b and d by the direction of stellar axial rotation. Therefore, in respect to the

observed variability of the crossover effect, we can discern between the two cases, (*a* and *b* or *c* and *d*). However, for the slowly rotating HD 187474 with $v_e = 0.06\,\mathrm{km\,s^{-1}}$ inferred from the known values of stellar rotational period and radius (Hubrig et al. 2000), the modelled variations are of small amplitude and, consequently, we are not able to distinguish between two cases due to the large errors in measurements of the crossover effect.

The corresponding simulated curves of the magnetic field characteristics variability are depicted in Fig. 1 by solid lines. These parameters (4) indicate that the magnetic field strength is approximately equal to $B_p = 9.7$ kG and $B_n = 12.8$ kG at the positive and negative dipole poles located on the stellar surface at the places with coordinates $\lambda_p = 6°$, $\delta_p = -54°$ and $\lambda_n = 188°$, $\delta_n = 51°$, respectively. The weaker positive pole turns to the observer at phase $\varphi = 0$. The reconstructed magnetic dipole, which could produce the observable configuration of the surface magnetic field, has a size of about $2a = 0.035\,R_\star$ with its centre shifted from the centre of the star by $a_0 = 0.055\,R_\star$. In Fig. 2 a schematic model of HD 187474 is shown for the phase $\varphi = 0.46$. Locations of the positive and negative virtual magnetic charges are marked by "+" and "–" signs, respectively. All the distances have the same scale.

As a next step, we excluded from the analysis the mean magnetic filed modulus observations (Mathys et al. 1997) marked by asterisks in Fig. 1, as they were obtained with a different instrumental configuration than the rest of the data, as well as the earliest (HJD = 2447287.859, rotational phase 0.223) measurement which falls apparently outside the sequence of the rest of observations. Then we repeated the χ^2 minimization procedure with $N_z = 52$ and $N_s = 33$. The best fit was obtained with the following parameters

$$\begin{cases} B_0 = 158 \pm 15\ \mathrm{kG}; & i = 89° \pm 5°; \\ a_1 = 0.043 \pm 0.002; & a_2 = 0.072 \pm 0.003; \\ \lambda_1 = 196° \pm 5°; & \delta_1 = 6° \pm 16°; \\ \lambda_2 = 193° \pm 3°; & \delta_2 = 27° \pm 4°, \end{cases} \quad (6)$$

and produced a minimum of χ^2-function at 4.61 (with the corresponding values of $\chi^2_z = 5.74$ and $\chi^2_s = 3.48$). The given parameters lead to the magnetic field strength of about $B_p = 9.7$ kG and $B_n = 12.8$ kG at the positive and negative dipole poles on the stellar surface, with the coordinates $\lambda_p = 6°, \delta_p = -54°$ and $\lambda_n = 187°, \delta_n = 50°$. The reconstructed magnetic dipole, which could produce such surface magnetic filed configuration, has a size of about $2a = 0.035\,R_\star$ and its centre is shifted from the centre of the star by approximately $a_0 = 0.055\,R_\star$. Considering the values of the best-model parameters (6), the magnetic dipole axis crosses the rotational axis at the angle $\beta = 37° \pm 17°$ (A.12). The errors of the best-model parameters (6) are inter-dependent because they are determined from the available observational uncertainties by applying the least-square technique. Therefore, we can suppose that the accuracy of the estimation of β in the MCD method is the same as the accuracy of parameters in the best model (6). The searched accuracy can be obtained from an averaged contribution of each parameter's uncertainty to the error of β according to (A.12).

Omission of the data for the mean longitudinal field obtained by Mathys (1991) and Mathys & Hubrig (1997) in the both previous steps does not change significantly the values of the parameters (4, 6) of the best-fit model and slightly reduces χ^2: 5.78 and 4.28 in the first and the second step, respectively.

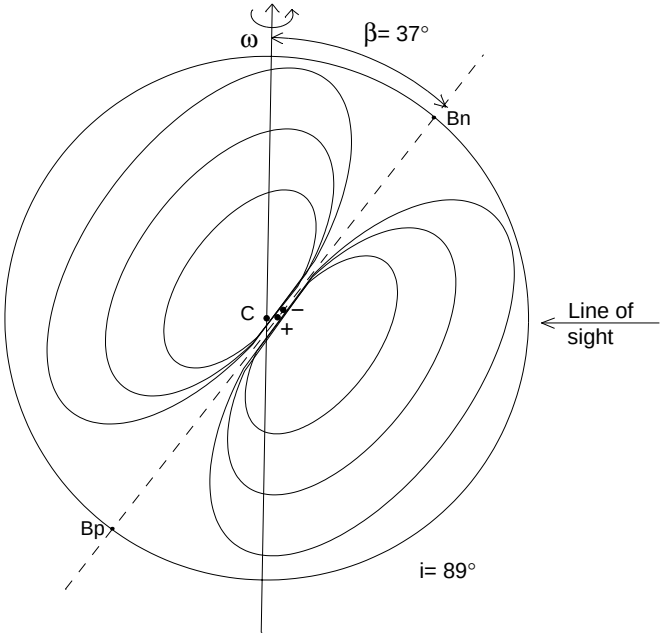

Fig. 2. Model of HD 187474 with the magnetic field structure for the phase of stellar rotation $\varphi = 0.46$. The axes of stellar rotation and magnetic dipole are traced by solid and dashed line, respectively. All the distances have the same scale.

The relatively poor agreement of the simulated curve with the observational data of the magnetic field modulus around phase $\varphi = 0.5$ stems from the problem of simultaneous occurence of the high value of the longitudinal magnetic field and the low value of the magnetic field modulus for this particular phase. In this phase interval there are significantly more measurements of B_z than B_s. Consequently, the weight of the longitudinal field measurements is higher, according to (3). As a result we observe some discrepancy of the simulated curve with the magnetic field modulus data while the longitudinal field data are described relatively well.

In the case of a decentered magnetic dipole presented here, the surface magnetic field can not be adequately described with the dipole moment only. As it was recently shown by Landstreet & Mathys (2000), for HD 187474 the quadrupole and octupole components should be taken into account. In the model with the dipole, quadrupole and octupole components the *magnetic moment* is proportional to the charge of virtual magnetic sources, while its dependence on their separation is non-linear (Landau & Lifshits 1988). It means that after change of the values of virtual magnetic charges and corresponding change of their separation in order to provide the assumed constancy of the magnetic moment, new configuration of the surface magnetic field will be different from the previous one. Thereby, in the applied model the distribution of magnetic field on the stellar surface depends on the dipole size (or separation of the virtual magnetic charges). Both best-fit sets (4 and 6), do not differ significantly (taking into account the estimation

errors) and indicate that for HD 187474 the magnetic dipole is decentered from the stellar centre by 0.055 $R_\star$ and has an approximate size 0.035 $R_\star$.

2.3. Comparison with the previous results

Configuration of the surface magnetic field of HD 187474 was recently modelled by Bagnulo et al. (2002) in the frame of the multipole model as a superposition of an arbitrarily oriented central magnetic dipole and non-linear quadrupole which operates with 10 free parameters. Analysing the observational data of the four characteristics of magnetic field (mean longitudinal magnetic field, crossover effect, mean surface magnetic field modulus and mean quadratic field), they obtained the best fit, $\chi^2 = 3.82$, for the following values of $i = 97.^\circ5$, $\beta = 79.^\circ9$, $B_\mathrm{d} = 6.4$ kG, $B_\mathrm{q}/B_\mathrm{d} = 1.094$, $v_\mathrm{e} = 0.06\,\mathrm{km\,s^{-1}}$ (Bagnulo 2002). Excluding the mean quadratic field data and the mean magnetic field modulus data from the analysis they were able to reduce $\chi^2 = 3.59$ and $\chi^2 = 3.36$ respectively. A remarkable feature of this model is related to the comparatively high, close to unity, ratio of the quadrupole field strength to the dipole field strength.

Comparing our results (4, 6) with those of Bagnulo (2002), one may note the relatively close values of the inclination i (i.e., $i = 89^\circ$ and $i = 97.5^\circ$), and the disagreement in the values of β (i.e., $\beta = 37^\circ$ and $\beta = 79.9^\circ$). However, we mention that in the MCD approach we work with the magnetic dipole (centered or decentered) with β completely[1] specifying the angle between the rotational and magnetic axes, while in the multipole approach of Bagnulo et al. (1996), β defines the central magnetic dipole orientation, without any information on the quadrupole (and octupole) orientation.

In the special case of HD 187474, where the multipole model shows existence of the quadrupole magnetic field of approximately the same strength as the dipole one (Bagnulo et al. 2002), one can hardly expect a good agreement between the β estimates in both methods. A coincidence in β could be achieved if both approaches operate with a centered symmetric magnetic dipole only. Nevertheless, similar values of β can also be obtained from the MCD method and multipole model with co-linear dipole, quadrupole and octupole components (Landstreet & Mathys 2000).

The inclusion of the observations of the crossover effect into analysis decreases the χ^2 minimum value (2), because the data have comparatively high observational errors. For the available crossover effect data $N_\mathrm{c} = 20$ with our best-fit model parameters (4) and the equatorial velocity $v_\mathrm{e} = 0.06\,\mathrm{km\,s^{-1}}$ (Hubrig et al. 2000) we obtain a reduced $\chi^2_\mathrm{c} = 1.25$. Such a small value of χ^2_c leads to the averaged $\chi^2 = 4.49$ and $\chi^2 = 3.49$ at the first and second steps, respectively, and to $\chi^2 = 3.21$ when omitting the mean longitudinal field data obtained by Mathys (1991) and Mathys & Hubrig (1997) (see Sect. 2.2). We note that in the two above mentioned steps we analysed the $N_\mathrm{z} = 52$ available observations of the mean longitudinal magnetic field, while in the paper of Bagnulo et al. (2002) the authors used 20 values. Hence, both approaches provide approximately the same quality of the best fitted curves (see Fig. 1). Besides, our estimations of $\beta = 37^\circ$ and $i = 89^\circ$ are comparable with the results of Landstreet & Mathys (2000) for HD 187474 (see Table 1 in their paper). We note also that our simulated curve fits well the recent observations of the mean quadratic magnetic field B_mq (Landstreet & Mathys 2000), as marked by open squares in the right bottom panel of Fig. 1.

[1] If the magnetic dipole axis intersects the stellar rotation axis (see Appendix A).

3. Discussion

As follows from the comprehensive analysis of Donati et al. (1997), the magnetic signatures detected on cool stars show, in general, several sign reversals throughout the line profile, indicating that the surface field structure is rather complex. Besides, mapping of the surface magnetic field for AB Dor (Donati et al. 1999) apparently shows a complex field configuration (there are rings and bows of the maximum azimuthal and radial magnetic field intensity). It is evident that such a complex surface magnetic field configuration is not easy to reproduce in the frame of the simplistic model of a centered magnetic dipole. Higher magnetic moments must be included for the CP stars, as well as for the cool stars (Landstreet & Mathys 2000). The model proposed in this paper represents an alternative to the approaches of Bagnulo et al. (1996) and Landstreet & Mathys (2000). It leads to the same agreement between the simulated and observed magnetic field data for HD 187474, as the model with a superposition of the dipole and non-linear quadrupole fields, that is much better than the agreement in the approach of Landstreet & Mathys (2000). At the same time, the point field source model is relatively simpler, as it operates with a smaller amount of free parameters (A.5) than the approach of Bagnulo et al. (1996). This finding is a contribution of this work.

HD 187474 shows no evidence of high-overtone pulsations in the Cape Survey (Martinez & Kurtz 1994). The lack of the high-overtone pulsations is associated with the comparatively high effective temperature $T_\mathrm{eff} = 10\,090 \pm 180$ K obtained for HD 187474 (Hubrig et al. 2000), that is evidently hotter than all known roAp stars. Besides, this fact could be explained partly in terms of the model applied, which shows that negative and positive dipole poles have the latitudes $\delta_\mathrm{n} = 51^\circ$ and $\delta_\mathrm{p} = -54^\circ$, respectively, while inclination of the rotational axis to the line of sight is $i = 89^\circ$. Consequently, as the star rotates, the observer never looks directly at the magnetic poles and can not detect the photometric pulsations of a sufficiently high amplitude even if they were present in HD 187474.

A similar surface magnetic field structure was obtained recently by Glagolevskij & Gerth (2002) for another Ap star, CU Virginis, on the basis of the longitudinal field measurements. They also revealed that observations can be described sufficiently well within the model of a decentered dipole only. These authors supposed that the complex structure of the surface magnetic field could be related to the young age of CU Vir, which was recently formed as a magnetic CP star after arriving at the Zero Age Main Sequence (ZAMS) (Glagolevskij & Chountonov 1998). In contrast to CU Vir, HD 187474 has already spent a 0.69 fraction of its main-sequence life (Hubrig et al. 2000). Besides the ages, these

two stars differ significantly in the rotational period – 2345 d for HD 187474 and 0.52 d for CU Vir (Pyper et al. 1998). Respectively, presence of a complex magnetic field configuration at the stellar surface can not be recognized as an indicator that the star has just started its life on ZAMS as a magnetic star (such an assumption needs still a comprehensive study).

In any case, the apparent shift of the magnetic dipole from the stellar centre obtained here for HD 187474 and for CU Virginis (Glagolevskij & Gerth 2002) and its possible size (of about $0.035\,R_\star$ as it is for HD 187474) should be taken into account while considering the stellar evolution paths. Present fossil and core-dynamo theories cannot explain well all the problems of the magnetic Ap and Bp stars (Moss 2001), and investigation of the surface structure of magnetic field could shed an additional light on problems of the CP stars.

Appendix A: Field of a magnetic dipole

To model the structure of the surface magnetic field produced by a magnetic dipole (mathematically formulated with help of two virtual magnetic charges arbitrarily located in the stellar interior), we apply the exact expression for the orthogonal components of the magnetic field vector (see Khalack et al. 2001a):

$$\left\{\begin{array}{rcl} B_x = & \dfrac{Q_\mathrm{r}}{R_\star^2} & \left[\dfrac{(\sin\theta\cos\psi - a_1\sin\theta_1\cos\psi_1)}{\left(1+a_1^2-2a_1D_1\right)^{3/2}}\right. \\ & & \left. -\dfrac{(\sin\theta\cos\psi - a_2\sin\theta_2\cos\psi_2)}{\left(1+a_2^2-2a_2D_2\right)^{3/2}}\right]; \\ B_y = - & \dfrac{Q_\mathrm{r}}{R_\star^2} & \left[\dfrac{(\sin\theta\sin\psi - a_1\sin\theta_1\sin\psi_1)}{\left(1+a_1^2-2a_1D_1\right)^{3/2}}\right. \\ & & \left. -\dfrac{(\sin\theta\sin\psi - a_2\sin\theta_2\sin\psi_2)}{\left(1+a_2^2-2a_2D_2\right)^{3/2}}\right]; \\ B_z = & \dfrac{Q_\mathrm{r}}{R_\star^2} & \left[\dfrac{(\cos\theta - a_1\cos\theta_1)}{\left(1+a_1^2-2a_1D_1\right)^{3/2}}\right. \\ & & \left. -\dfrac{(\cos\theta - a_2\cos\theta_2)}{\left(1+a_2^2-2a_2D_2\right)^{3/2}}\right], \end{array}\right. \tag{A.1}$$

where

$$\left\{\begin{array}{l} D_1 = \sin\theta\sin\theta_1\cos(\psi-\psi_1) + \cos\theta\cos\theta_1; \\ D_2 = \sin\theta\sin\theta_2\cos(\psi-\psi_2) + \cos\theta\cos\theta_2. \end{array}\right. \tag{A.2}$$

Here Q_r and a_1, a_2 specify the modulus of magnetic charges and their distances from the centre of the star, expressed in the units of stellar radius $R_\star$ (see Fig. 1 in Khalack 2002). The variables (θ_1, ψ_1) and (θ_2, ψ_2) determine the angular coordinates of the two magnetic charges in the spherical reference frame related to the observer. It should be noted that coordinates (θ, ψ) of an arbitrary point on the stellar surface are linked to their angular coordinates (δ, λ) in the spherical reference frame related to the star by the following expressions (Khalack et al. 2001a):

$$\left\{\begin{array}{l} \cos\theta = \sin\delta\cos i + \cos\delta\sin i\cos(\varphi+\lambda), \\ \sin\theta = \sqrt{1-\cos^2\theta}; \end{array}\right. \tag{A.3}$$

and

$$\left\{\begin{array}{l} \cos(\psi-\Omega) = \dfrac{\sin\delta - \cos i\cos\theta}{\sin\theta\sin i}, \\ \sin(\psi-\Omega) = \cos\delta\,\dfrac{\sin(\varphi+\lambda)}{\sin\theta}, \end{array}\right. \tag{A.4}$$

where indexes are omitted for the simplicity.

It is desirable to operate initially within the model with the coordinates related to the star (δ, λ). Therefore, in order to describe configuration of the surface magnetic field, we determine eleven free model parameters (taking into account the form of the weighting function (1)):

$$\left\{\begin{array}{l} B_0 = Q_\mathrm{r}/R_\star^2; \\ 0 \le a_1, a_2 < 1; \\ 0 \le u_\mathrm{c}, u_\mathrm{l} \le 1; \\ 0^\circ \le i < 180^\circ; \\ 0^\circ \le \lambda_1, \lambda_2, \Omega < 360^\circ; \\ -90^\circ \le \delta_1, \delta_2 \le 90^\circ. \end{array}\right. \tag{A.5}$$

Two of them, (Ω, i) specify the position of the rotational axis of the star with respect to the observer, next three $(u_\mathrm{c}, u_\mathrm{l}, B_0)$ characterize the star and the virtual charge, and the remaining six specify the positions of point-like sources of the field in the stellar interior. The quantity B_0 is expressed in Gauss (G) and is physically proportional to the magnetic field strength at the dipole's pole (on the stellar surface) for the case of the centered symmetric magnetic dipole.

Sometimes it is useful to estimate the surface magnetic field strength at the dipole's poles. For an arbitrarily located (and oriented) magnetic dipole the coordinates of its poles (in the spherical reference frame related to the star) could be expressed via the coordinates of the two magnetic charges in the following way:

$$\left\{\begin{array}{rcl} \sin\delta_\mathrm{p} & = & a_1(1+\eta_\mathrm{p})\sin\delta_1 - a_2\eta_\mathrm{p}\sin\delta_2; \\ \cos\delta_\mathrm{p}\sin(\varphi+\lambda_\mathrm{p}) & = & a_1(1+\eta_\mathrm{p})\cos\delta_1\sin(\varphi+\lambda_1) \\ & & -a_2\eta_\mathrm{p}\cos\delta_2\sin(\varphi+\lambda_2); \\ \cos\delta_\mathrm{p}\cos(\varphi+\lambda_\mathrm{p}) & = & a_1(1+\eta_\mathrm{p})\cos\delta_1\cos(\varphi+\lambda_1) \\ & & -a_2\eta_\mathrm{p}\cos\delta_2\cos(\varphi+\lambda_2); \end{array}\right. \tag{A.6}$$

in the case of the positive pole with coordinates $(\lambda_\mathrm{p}, \delta_\mathrm{p})$ and

$$\left\{\begin{array}{rcl} \sin\delta_\mathrm{n} & = & a_2(1+\eta_\mathrm{n})\sin\delta_2 - a_1\eta_\mathrm{n}\sin\delta_1; \\ \cos\delta_\mathrm{n}\sin(\varphi+\lambda_\mathrm{n}) & = & a_2(1+\eta_\mathrm{n})\cos\delta_2\sin(\varphi+\lambda_2) \\ & & -a_1\eta_\mathrm{n}\cos\delta_1\sin(\varphi+\lambda_1); \\ \cos\delta_\mathrm{n}\cos(\varphi+\lambda_\mathrm{n}) & = & a_2(1+\eta_\mathrm{n})\cos\delta_2\cos(\varphi+\lambda_2) \\ & & -a_1\eta_\mathrm{n}\cos\delta_1\cos(\varphi+\lambda_1); \end{array}\right. \tag{A.7}$$

in the case of the negative pole with coordinates $(\lambda_\mathrm{n}, \delta_\mathrm{n})$. Here the variables η_p and η_n are determined as:

$$\left\{\begin{array}{l} \eta_\mathrm{p} = \dfrac{\sqrt{\omega} - a_1(a_1 - a_2\Delta)}{a_1^2 + a_2^2 - 2a_1a_2\Delta}; \\ \eta_\mathrm{n} = \dfrac{\sqrt{\omega} - a_2(a_2 - a_1\Delta)}{a_1^2 + a_2^2 - 2a_1a_2\Delta}, \end{array}\right. \tag{A.8}$$

where

$$\begin{cases} \omega = a_1^2 a_2^2 (1-\Delta^2) + a_1^2 + a_2^2 - 2a_1 a_2 \Delta; \\ \Delta = \sin\theta_1 \sin\theta_2 \cos(\psi_1 - \psi_2) + \cos\theta_1 \cos\theta_2. \end{cases} \quad (A.9)$$

The coordinates of the dipole's poles $(\theta_p, \psi_p; \theta_n, \psi_n)$ are linked with their angular coordinates $(\delta_p, \lambda_p; \delta_n, \lambda_n)$ in the spherical reference frame related to the star by Eqs. (A.3), (A.4), where indexes p and n, related to the positive and negative poles, respectively, are omitted. Substituting by the positive pole coordinates (θ_p, ψ_p) or negative pole coordinates (θ_n, ψ_n) the arbitrary surface point coordinates (θ, ψ) in Eq. (A.1), we can determine the magnetic field modulus as $B_s = \sqrt{B_x^2 + B_y^2 + B_z^2}$ at the both poles of the magnetic dipole.

In order to estimate the magnetic dipole displacement relative to the centre of the star, we use instead of a_1 and a_2 the variables a_0 and a, that specify the distance of the dipole from the stellar centre and the half of the distance between the two magnetic charges, respectively, and are determined in the following way:

$$\begin{cases} a_0^2 = \left(a_1^2 + a_2^2 + 2a_1 a_2 F\right)/4; \\ a^2 = \left(a_1^2 + a_2^2 - 2a_1 a_2 F\right)/4, \end{cases} \quad (A.10)$$

where F specifies the cosine of angle between the directions from stellar centre to the locations of both magnetic charges:

$$\begin{aligned} F^2 = {} & 1 - \cos^2\delta_1 \cos^2\delta_2 \sin^2(\lambda_1 - \lambda_2) \\ & - \sin^2\delta_2 \cos^2\delta_1 - \sin^2\delta_1 \cos^2\delta_2 \\ & + 2\sin\delta_1 \cos\delta_1 \sin\delta_2 \cos\delta_2 \cos(\lambda_1 - \lambda_2). \end{aligned} \quad (A.11)$$

The corresponding value of the angle between the stellar rotation axis and the magnetic dipole axis can be determined as

$$\cos\beta = (a_1 \sin\delta_1 - a_2 \sin\delta_2)/2a. \quad (A.12)$$

In a general case, β specifies the angle between the vectors directed along the axes mentioned above. There is a possibility, for the model with a decentered magnetic dipole, that the dipole axis does not cross the rotational one in a three dimensional (3D) space. If these two axes have an intersection point, then the condition $\lambda_1 = \lambda_2 \pm n\pi$ with $n = 0, 1$ (if $\lambda_1 = \lambda_2$, then $a_1 \cos\delta_1 \neq -a_2 \cos\delta_2$) should be valid within the estimated errors.

Acknowledgements. Authors are kindly grateful to Prof. J. D. Landstreet and Dr. S. Bagnulo for fruitful discussions and valuable advices. We also thank Prof. S. V. Marchenko for careful reading of the manuscript and constructive remarks. Special thanks is due the referee who helped to significantly improve the paper. This work was partly supported by the VEGA grant No. 3014.

References

Bagnulo, S., Landolfi, M., & Landi Degl'Innocenti, M. 1996, A&A, 308, 115
Bagnulo, S. 2002, private communication
Bagnulo, S., Landi Degl'Innocenti, M., Landolfi, M., & Mathys, G. 2002, A&A, 394, 1023
Budaj, J. 1999, MNRAS, 310, 419
Didelon, P. 1987, The Messenger, 49, 5
Donati, J.-F., Semel, M., Carter, B. D., Rees, D. E., & Cameron, A. C. 1997, MNRAS, 291, 658
Donati, J.-F., Collier Cameron, A., Hussain, G. A. J., & Semel, M. 1999, MNRAS, 302, 437
ESA 1997, The Hipparcos and Tycho Catalogues, ESA Sp-1200
Gerth, E., Glagolevskij, Yu. V., & Sholz, G. 1997, in Stellar Magnetic Fields, ed. Yu. V. Glagolevskij, & I. I. Romanyuk (Moscow), 67
Glagolevskij, Yu. V., & Chountonov, G. A. 1998, Bull Spec. Astrophys. Obs., 45, 105
Glagolevskij, Yu. V., & Gerth, E. 2002, A&A, 382, 935
Hensberge, H. 1993, Long term variability in CP stars, in Peculiar versus normal phenomena in A-type and related stars, IAU Colloq. 138, ed. M. M. Dworetsky, F. Castelli, & R. Faraggiana, Astron. Soc. Pac. Conf. Ser., 44, 547
Hubrig, S., North, P., & Mathys, G. 2000, ApJ, 539, 352
Khalack, V. R., Khalack, Yu. N., Shavrina, A. V., & Polosukhina, N. S. 2001a, AZh, 78, N7, 655
Khalack, V. R., Khalack, Yu. N., Shavrina, A. V., & Polosukhina, N. S. 2001b, in Magnetic Fields Across the Hertzsprung-Russel Diagram, ed. G. Mathys, S. K. Solanki, & D. T. Wickramasinghe (San Francisco: ASP), 329
Khalack, V. R. 2002, A&A, 385, 986
Landau, L. D., & Lifshits, E. M. 1988, The classical Theory of Fields, vol. 2, 7th edition (Moscow), 510
Landstreet, J. D., & Mathys, G. 2000, A&A, 359, 213
Leeman, S. 1964, Mon. Not. Astr. Soc. South Africa, 23, 6
Nelder, A. J., & Mead, R. 1965, Computer Journal, 7, 308
Martinez, P., & Kurtz, D. W. 1994, MNRAS, 271, 129
Mathys, G. 1991, A&AS, 89, 121
Mathys, G. 1995a, A&A, 293, 733
Mathys, G. 1995b, A&A, 293, 746
Mathys, G., & Hubrig, S. 1997, A&AS, 124, 475
Mathys, G., Hubrig, S., Landstreet, J. D., Lanz, T., & Manfroid, J. 1997, A&AS, 123, 353
Moss, D. 2001, in Magnetic Fields Across the Hertzsprung-Russel Diagram, ed. G. Mathys, S. K. Solanki, & D. T. Wickramasinghe (San Francisco: ASP), 305
Press, W. H., Teukolsky, S. A., Vetterling, W. T., & Flannery, B. P. 1992, Numerical recipes in C: the art of scientific computing, 2nd ed. (Cambridge University Press), 995
Pyper, D. M., Ryabchikova, T., Malanushenko, V., et al. 1998, A&A, 339, 822
Schaller, G., Schaerer, D., Meynet, G., & Maeder, A. 1992, A&AS, 96, 269
Strasser, S., Landstreet, J. D., & Mathys, G. 2001, A&A, 378, 153